Femtosecond intersubband relaxation and population inversion in stepped quantum well

C. Y. Sung[a] and T. B. Norris
Center for Ultrafast Optical Science, 1006 2200 Bonisteel Blvd./IST, Ann Arbor, Michigan 48109

A. Afzali-Kushaa and G. I. Haddad
EECS Department, The University of Michigan, Ann Arbor, Michigan 48109

(Received 9 June 1995; accepted for publication 12 November 1995)

We have investigated intersubband relaxation rates in a stepped quantum well at room temperature using differential transmission spectroscopy with subpicosecond time resolution. The dynamics of the subband populations are derived from the experimentally observed reduction of oscillator strength of the corresponding exciton transitions. In the stepped quantum well the relaxation through longitudinal optical-phonon emission from $n=3$ to 1 (25 ps) is slower than that from 2 to 1 (220 fs), due to the reduced wave function overlap and larger wave vector required for intersubband scattering. When the $n=3$ state is pumped, a population inversion between *n3* and *n2* (which are separated by 7 THz) is observed. © *1996 American Institute of Physics.* [S0003-6951(96)02404-3]

The generation of coherent far-infrared radiation (FIR) in superlattices or multiple-quantum well (MQW) structures has been a goal for many years.[1] The use of intersubband transitions to generate coherent far-infrared radiation was first successfully demonstrated by J. Faist *et al.*,[2] with a lasing wavelength of 4 μm in quantum cascade lasers. However, new structures are needed to generate radiation in the 30–300 μm regime (1–10 THz). In this letter, we demonstrate how a stepped quantum well structure can modify the intersubband relaxation rates, allowing a population inversion between subbands to be achieved.[3,4] We measured the intersubband relaxation rates in the stepped quantum well with femtosecond differential transmission spectroscopy and experimentally observed the population inversion.

The stepped QW structure is shown in the inset of Fig. 1. The basic idea is to design the structure so that it can behave as a four-level laser system, with a population inversion between levels 3 and 2.[4] A pump laser (CO_2 laser or other IR source) would be used to excite a doped QW, pumping carriers from subband 1 to subband 4 or higher subbands. The energy separation between subband 4 and subband 3 is designed to be greater than the longitudinal optical-(LO)phonon energy; thus the excited carriers will relax very fast (within 500 fs) to subband 3.[5–7] The dominant relaxation mechanism for relaxation from subband 4 to 3 is polar LO-phonon scattering, which is proportional to the wave function overlap and inversely proportional to the square of the phonon wave vector involved.[8,9] Thus relaxation to subband 3 will be faster than to the other subbands 2 or 1. By tailoring the well width, barrier width, and the Al composition of the step region, we can design the energy separation between subband 2 and 1 to be larger than the LO-phonon energy, while the 3-2 separation is less than the LO-phonon energy. The carriers in subband 2 will be depopulated very fast to level 1 through LO-phonon relaxation; however, the 3 to 2 scattering rate will be significantly reduced.[10,11] Furthermore, the wave function overlap between levels 2 and 1 is larger than the overlap between level 3 and 1, and a larger wave vector is required for intersubband scattering from level 3 to level 1 than for 2 to 1. Thus carrier relaxation via LO-phonon emission from $n=2$ to 1 will be much faster than from 3 to 1.

From calculations of the intersubband relaxation rates including LO- and longitudinal acoustic-(LA-)phonon scattering, we find relaxation times $\gamma_{31}^{-1}\approx 15$ ps, $\gamma_{32}^{-1}\approx 1$ ns, $\gamma_{21}^{-1}\approx 500$ fs for $k=0$.[4] To measure these intersubband relaxation times experimentally, we have used deferential transmission spectroscopy with femtosecond resolution, pumping and probing across the band gap.[5] Two white-light continuum pulses are generated using a 250 kHz, 3.5 μJ, 85 fs Ti:sapphire amplifier.[12] A fraction from one of the continua, ranging from 1.4 to 1.65 eV is used as a broadband probe pulse. The dispersion of the broadband probe was compensated by double-pass prism pairs so that transmission spectra

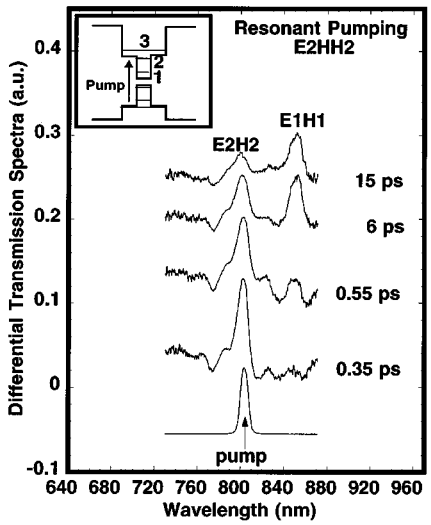

FIG. 1. Time-resolved DTS with resonant E2HH2 excitation at time delays of 0.35, 0.55, 6, and 15 ps. The peaks correspond to the exciton transitions bleached by pump-induced carriers.

[a]Electronic mail: chunyung@engin.umich.edu

of the entire near-band-edge region could be obtained with 120 fs resolution. A 10 nm bandwidth filter was used to select the pump pulse wavelength from the other continuum pulse. An optical multichannel analyzer (OMA) was used to measure differential transmission spectra (DTS).

The stepped quantum well sample, grown by molecular beam epitaxy, consisted of 20 periods of 100 Å GaAs wells which are surrounded by 150 Å $Al_{0.15}Ga_{0.85}As$ step layers and 100 Å $Al_{0.25}Ga_{0.75}As$ cladding layers. The GaAs substrate was removed over an area of $\approx 2\times 2$ mm^2 by selective etching to allow optical transmission measurements. The positions of the excitonic peaks in DTS agreed well with calculated values. The calculated subband splitting between the first and second electronic subband is about 68 meV, almost equal to two times the LO-phonon energy. The second and third electronic subband splitting is about 28 meV, smaller than the LO-phonon energy.

In the valence band, the subbands are neither isotropic nor parabolic due to the band mixing. Thus the scattering rate expressions for holes are more complicated than in the conduction band case. However, Hopfel *et al*. have measured a very long relaxation time from HH2 to HH1 (HH, LH, and *E* mean heavy hole band, light hole band, and conduction band; the number represents subband index) about 130 ps when the heavy hole subband splitting is smaller than the LO-phonon energy.[11] Thus electronic relaxation in the conduction band will dominate the time evolution of the DTS signal at early time. Furthermore, the contribution to the DTS bleaching is much less than the electron due to the much larger density of states in the valence band.

We performed the measurement at room temperature without doping or bias. In the case of low optical density ($-\Delta\alpha d \ll 1$), the normalized transmission changes $\Delta T/T_0$ are approximately equal to $-\Delta\alpha d$. The changes of the reflectivity are not included, since those changes which were measured by differential reflection spectra were smaller than 5% of the DTS signal.[13] In Ref. 14, it has been demonstrated that the DTS integrated over the exciton peak associated with a given subband is proportional to the carrier density in that subband when the carrier density is below 10^{12} cm^{-2}. The differential transmission versus pumping fluence for our sample is plotted in the inset of Fig. 4; the bleaching signal integrated over one transition peak depends almost linearly on carrier density. Therefore, the integrated DTS can be used as a direct measure of the subband population since the signal is proportional to the number density in each subband.[15]

In Fig. 1, we show a series of DTS, where the pump has been tuned to resonantly excite the E2HH2 transition. Only a small signal from the E3HH3 transition is observable in the DTS, since we directly pump the E2HH2 exciton. The small bump at 830 nm, is calculated to be the E1HH3 transition. The E1HH1 exciton peak also includes a small contribution from E1LH1. A total carrier density 5×10^{11} cm^{-2} is estimated from the pump power and spot size. The DTS show a peak at E2HH2 which has a fast partial decay as the E1HH1 peak rises. The spectrally integrated peak amplitudes are shown in Fig. 2. The inset gives a shorter time scale plot. The 220 fs decay of E2HH2 and associated rise of E1HH1 are

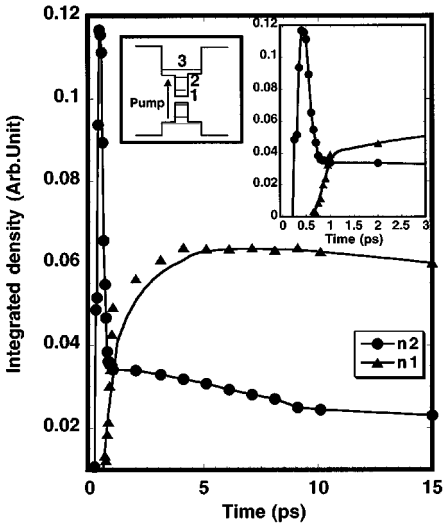

FIG. 2. Time evolution of the spectrally integrated DTS changes at E2HH2 and E1HH1 transitions from Fig. 1. The inset shows the data at early time (lines are guide to the eye).

attributed to the electronic relaxation between the second and first subband in the conduction band. This value is very close to the LO-phonon-mediated scattering time we calculated for our structure. The nonzero amplitude of the E2HH2 transition after the initial decay we attribute to the residual hole population in the HH2 valence band level.[5] The hole relaxation from HH2 to HH1 with 11 meV energy splitting is longer 100 ps. Due to poor interface quality in the stepped QW, we have interband carrier recombination rate faster than typical value. Thus E2HH2 and E1HH1 peaks show slow decays (about 80 ps) after the initial fast relaxation.

In Fig. 3, we show a series of DTS where the pump has been tuned to the E3HH3 transition. Initially, the E3HH3 signal rises with the integral of the pump pulse. Carriers are pumped directly into *n1* contribute to the initial fast rise of E1HH1. The spectrally integrated peak amplitudes are shown in Fig. 4. The fitting curves are obtained from solving the following coupled rate equations.

$$\frac{dN_3}{dt} = -\gamma_{31}N_3 - \gamma_{32}N_3 - \gamma_r N_3 + N_{30}g(t),$$

$$\frac{dN_2}{dt} = \gamma_{32}N_3 - \gamma_{21}N_2 - \gamma_r N_2 + N_{20}g(t),$$

$$\frac{dN_1}{dt} = \gamma_{21}N_2 + \gamma_{31}N_3 - \gamma_r N_1 + N_{10}g(t),$$

where *g(t)* is the pump pulse and N_{io} is the initial population in subband *i*. The best fit to the data has been obtained with relaxation times $\gamma_{31}^{-1}=25$ ps, $\gamma_{21}^{-1}=0.22$ ps, $\gamma_{32}^{-1}=31$ ps, and the carrier recombination time $\gamma_r^{-1}=75$ ps. Because of the reduced intersubband scattering rate from level 3 to level 1, γ_{31}^{-1} shows a much slower decay 25 ps compared with the γ_{21}^{-1} fats decay 220 fs. Since the subband splitting (28 meV) between 3 and 2 is smaller than the LO-phonon energy (36 meV), γ_{32}^{-1} has a decay time 31 ps longer than γ_{21}^{-1}. However, γ_{32}^{-1} is still faster than the calculated value (1 ns) at

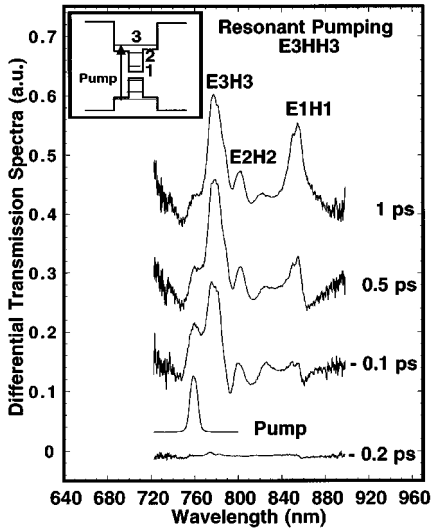

FIG. 3. Time-resolved DTS with resonant E3HH3 excitation taken at time delays of 0, 0.1, 0.5, and 1 ps. The peaks correspond to exciton transitions bleached by pump-induced carriers.

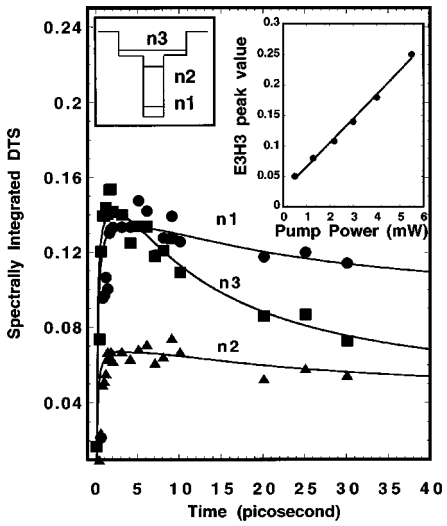

FIG. 4. Time evolution of the spectrally integrated DTS changes at E3HH3, E2HH2, and E1HH1 transitions from Fig. 3. The inset shows spectrally integrated DTS values of E3HH3 transition vs pump density. The lines are solutions to the coupled rate equations.

zone center ($k_{\|}=0$). We attribute this difference to the fast intersubband scattering of ($k_{\|}\neq 0$) electrons in the high-energy tail of the thermal carrier distribution in the $n-3$ subband at room temperature. (γ_{32} is strongly reduced at low temperature.) Thus electrons scattering from $n=3$ to 2 maintains a nonzero population in $n=2$, which remains nearly flat over the first 40 ps, as can be seen in Fig. 4. Since the total E3HH3 decay is on the order of 15 ps, significantly longer than the E2HH2 decay (220 fs), it is clear that the intersubband relaxation rates can be strongly modified in the stepped QW structure.

The oscillator strength is proportional to the square of the envelope function overlap integral. The calculated relative oscillator strengths for E3HH3, E2HH2, and E1HH1 are 1, 0.97, and 0.94, respectively.[15,16] Thus we could take both E2HH2 and E3HH3 transitions to have roughly equal oscillator strength. Because the E3HH3 peak is much larger than that of E2HH2 in Fig. 3, the E3HH3 decay time (15 ps) is much longer than that of E2HH2 (220 fs) and spectrally integrated DTS signals are proportional to each subband population, we can confirm the presence of a population inversion between the $n=3$ and $n=2$ levels. In fact, the population inversion is maintained during the entire decay of the total carrier population in the QW. This implies that we should be able to maintain a significant population inversion between levels 3 and 2 by continuously pumping carriers from the ground state to the third or higher subbands in a doped QW sample.

In summary, we have investigated intersubband relaxation rates in a stepped quantum well structure at room temperature using differential transmission spectroscopy with subpicosecond time resolution. Due to the reduced wave function overlap and larger wave vector required for intersubband scattering, the intersubband relaxation rates can be modified from a few hundred femtoseconds to a few tens of picoseconds in a stepped QW. Our data clearly show a fast electronic intersubband relaxation time of 220 fs from level 2 to level 1, slow relaxation times 25 ps for $3\rightarrow 1$ and 31 ps for $3\rightarrow 2$. Those measured time constants are consistent with our calculated values. A population inversion between levels $n=3$ and 2 separated by 7 THz has been observed for the first time to our knowledge. Optical pumping (CO_2 or other IR sources) from $n=1$ to $n\geqslant 3$ in doped structure should be able to generate FIR radiation in this stepped quantum well structure.

This work was supported by the National Science Foundation through the Center for Ultrafast Optical Science under STC PHY 8920108 and in part by the U.S. Army Research Office under Grant No. DAAL03-92-G-0109.

[1] R. F. Kazarinov and R. A. Suris, Sov. Phys. Semicond. **5**, 707 (1971).
[2] J. Faist, F. Capasso, D. L. Sivco, C. Sirori, A. L. Hutchinson, and A. Y. Cho, Science **264**, 533 (1994).
[3] T. B. Norris and C. Y. Sung, Postdeadline Paper PDP3, in Proceedings of the OSA Topical Meeting on Ultrafast Electronics and Optoelectronics, Dana Point, CA, 1995 (unpublished).
[4] A. Afzali-Kushaa, G. I. Haddad, and T. B. Norris, IEEE J. Quantum Electron. **31**, 135 (1995).
[5] S. Hunsche, K. Leo, H. Kurz, and K. Kohler, Phys. Rev. B **50**, 5791 (1994).
[6] J. Faist, F. Capasso, D. L. Sivco, C. Sirori, A. L. Hutchinson, S. N. G. Chu, and A. Y. Cho, Appl. Phys. Lett. **63**, 1354 (1993).
[7] R. Ferreira and G. Bastard, Phys. Rev. B **40**, 1074 (1989).
[8] J. A. Brum and G. Bastard, Phys. Rev. B **33**, 1420 (1986).
[9] J. A. Brum, T. Weil, J. Nagle, and B. Vinter, Phys. Rev. B **34**, 2381 (1986).
[10] D. Y. Oberli, D. R. Wake, M. V. Klein, J. Klem, T. Henderson, and H. Morkoc, Phys. Rev. Lett. **59**, 696 (1987).
[11] R. A. Hopfel, R. Rodrigues, Y. Iimura, T. Yasui, Y. Segawa, Y. Aoyagi, S. M. Goodnick, and M. C. Tatham, Phys. Rev. B **47**, 10943 (1993).
[12] T. B. Norris, Opt. Lett. **17**, 1099 (1992).
[13] S. Hunsche, H. Heesel, and H. Kurz, Opt. Commun. **109**, 258 (1994).
[14] S. Hunsche, K. Leo, and H. Kurz, Phys. Rev. B **49**, 16565 (1994).
[15] L. Banyai and S. W. Koch, Z. Phys. B. Condens. Matter **63**, 283 (1986).
[16] J. Singh, *Physics of Semiconductors and Their Heterostructures*, (McGraw-Hill, New York, 1993), Appendix K.6.